Optimization of the Emitter's Bandgap and Thickness of AlxGa1-xAs/ GaAs Multi-junction Solar Cell

Abderrahmane. Hemmani*, Abdelkader Nouri*,**‡, Hamid Khachab*, Toufik Atouani*

* Department of Matter Sciences, Faculty of Exact Sciences, University of Mohammed TAHRI, BP 417 Bechar, 08000, ALGERIA

** LabMat Laboratory, BP 1523 EL-M'naouer Oran 31000, ALGERIA

(hemani1973@yahoo.fr , nouri_32@yahoo.fr, khachab_hamid_2000@yahoo.fr, toufikatouani1972@yahoo.fr)

‡ Corresponding author; Abdelkader NOURI, Department of Matter Sciences, Faculty of Exact Sciences, University of Mohammed TAHRI, BP 417, Bechar, 08000, Algeria,

Tel: +213 49238993, Fax: + 21349238974, nouri_32@yahoo.fr

Received: 11.09.2016 Accepted:20.12.2016

Abstract- In this paper an optimization model of the top cell emitter's bandgap and thickness of AlxGa1-xAs/ GaAs Multi-Junction Solar Cell (MJSC) is treated. This study allows to enhance, after two optimization steps, efficiency energy conversion up to 24.9% compared with existing studies. This model is based on the maximization of the smallest photocurrent over two solar cell junctions of the MJSC. The efficiency is boosted due to the limitation of the different types of photons' energy losses known in the GaAs solar cell materials.

Keywords Multi-junction Solar Cell; Bandgap; thickness; Photocurrent; Optimization; Efficiency; $Al_xGa_{1-x}As/GaAs$

1. Introduction

The Multi-junction solar cells are widely studied for their high efficiency in comparison with single-junction ones. However, despite this advantage of the former, it is characterized by certain losses such as intrinsic losses, due to photon excess energy ($h\nu>>Eg$) or to the unabsorbed photon ($h\nu<Eg$) [1-3]. To minimize these losses, there have been extensive studies which shed light on this field during the last decade [4-7].

Among the solutions to the reduction of these losses in solar cells the use of the tandem solar cells is adopted. In this case, when solar cells are placed, in a way that their energy gaps are in decreasing order from top to bottom; maximum absorption of photons is ensured [8-10].

In the present search the effect of the $Al_xGa_{1-x}As/GaAs$ top solar cell emitter's bandgap and thickness on photocurrent is chosen to improve efficiency energy conversion. The first step to increase the photocurrent is by varying the bandgap; accordingly the spectral response of the two cells changes effectively. The second step to improve more the photocurrent, considering the obtained optimum bandgap value, is by varying the top cell emitter's thickness. This latter allows more photon absorption. Both optimum obtained values of top solar cell emitter's bandgap and thickness lead to a better efficiency energy conversion.

2. Photocurrent Model

Figure 1 shows the schematic diagram of the tandem solar cell. The two junctions are deposited in a decreasing order of bandgap in order to allow the top solar cell to absorb the photons of high energy before the bottom cell. The remaining photons are absorbed by the second cell, this configuration avoid the energy loss by thermalization [11-13].

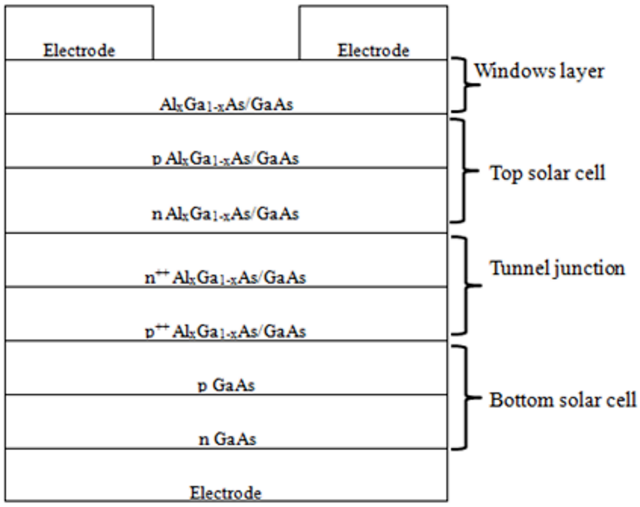

Fig. 1. Structure of the $Al_xGa_{1-x}As/GaAs$ tandem solar cell.

The following table summarizes the parameters of the two solar cells used to calculate photocurrent of the tandem solar cell showed in Fig.1 [14, 15].

In order to investigate the influence of the emitter's bandgap and thickness on the efficiency energy conversion in $Al_xGa_{1-x}As/GaAs$ tandem solar cell, the total photocurrent density J_{ph} in each cell is evaluated based on the total photocurrent density in standard p-n junction model.

J_{ph} is given by [16, 17]:

$$J_{ph}(\lambda) = J_p(\lambda) + J_n(\lambda) + J_d(\lambda) \qquad (1)$$

$J_p(A/m^2)$, $J_n(A/m^2)$ and $J_d(A/m^2)$in Eq.(1) are, respectively, the photocurrent density in p, n and depletion region.

The emitter photocurrent density is given by:

$$J_n = qD_n\left(\frac{dn_p}{dx}\right)_{\delta_p} \qquad (2)$$

Table 1. Parameters of the AlGaAs/GaAs tandem solar cell.

	Top cell	**Bottom cell**
Acceptor concentration (cm^{-3})	2.10^{17}	2.10^{17}
Donor concentration (cm^{-3})	2.10^{17}	2.10^{17}
Intrinsic concentration (cm^{-3})	2.10^{3}	$2.1x10^{6}$
Electron mobility ($cm^2\ V^{-1}\ s^{-1}$)	6000	9340
Hole mobility ($cm^2\ V^{-1}\ s^{-1}$)	200	450
Emitter thickness (µm)	Variable with x	1
Base thickness (µm)	1	1.5
Bandgap Eg (eV)	Variable with x	1.42

Which leads to the following expression:

$$J_n = \frac{qF(1-R)\alpha L_n}{\kappa^2 L_n^2 - 1} \times \left[\frac{\left(\frac{S_n L_n}{D_n} + \alpha L_n\right) - \exp(-\alpha x)\left(\frac{S_n L_n}{D_n}\cosh\frac{\delta_p}{L_n} + \sinh\frac{\delta_p}{L_n}\right)}{\frac{S_n L_n}{D_n}\sinh\frac{\delta_p}{L_n} + \cosh\frac{\delta_p}{L_n}} - \alpha L_n \exp(-\alpha\delta_p)\right] \qquad (3)$$

The signification of each parameter in Eq.(3) is explained in table 2.

Table 2. Signification of parameters in Eq.(3) to Eq.(6).

Parameters	Signification
q	The elementary charge
F	The incident photon flux at surface (W/m^2)
R	Reflection coefficient
α	Absorption coefficient (m^{-1})
$L_{n,p}$	The electron, hole diffusion length respectively(m)

$S_{n,p}$	The electron, hole surface recombination velocity respectively (m^{-2})
$D_{n,p}$	The electron, hole diffusion coefficient respectively(m^2/s)
$\delta_{p,n}$	The thickness of p, n region respectively (m)
x	Arbitrary position in p, n region
$\tau_{n,p}$	Electrons, holes lifetime respectively (s)

Where $L_n = \sqrt{D_n \tau_n}$

The photocurrent density in the depletion region is expressed by:

$$J_d = qF(1-R)\exp(-\alpha\delta_p)[1-\exp(-\alpha W)] \quad (4)$$

Where W is the depletion region thickness

The photocurrent density at base region is given by:

$$J_p = -qD_p\left(\frac{d\Delta p}{dx}\right)_{\delta_p + w} \quad (5)$$

Where Δp is the hole excess concentration (m^{-3})

Which leads to the following expression:

$$J_p = \frac{qF(1-R)\alpha L_p}{\kappa^2 L_p^2 - 1}\exp(-\alpha(\delta_p + w)) \times \left[\alpha L_p - \frac{\frac{S_p L_p}{D_p}\left[\cosh\frac{\delta_n}{L_p} - \exp(-\alpha\delta_n)\right] + \sinh\frac{\delta_n}{L_p} + \alpha L_p \exp(-\alpha\delta_n)}{\frac{S_p L_p}{D_p}\sinh\frac{\delta_n}{L_p} + \cosh\frac{\delta_n}{L_p}}\right] \quad (6)$$

Where $L_p = \sqrt{D_p \tau_p}$

The total photocurrent density J_{ph} is obtained by integrating the photocurrent density J_{ph} (λ) of Eq.(1) on the whole range of the AM 1.5 solar spectrum.

We note that the effect of windows layer and the tunnel junction are not considered in our photocurrent evaluation.

3. Results and Discussions

3.1. The spectral response

In order to associate the conversion energy efficiency to the photocurrent, it is very useful to show the spectral response range of each separate cell.

Figure 2 shows the variation of spectral response curves for a random x of $Al_xGa_{1-x}As/GaAs$ cell (Black) and for GaAs cell (Red). The photons of wavelength varies from 0.24 µm to 0.68µm are absorbed by the top solar cell, this is why the second's cell spectral response is weak in the aforementioned range.

The bottom cell's bandgap allows the absorption of photons in the range of wavelength from 0.68 µm to 0.87 µm meanwhile, the top solar is transparent. This phenomenon results of the exponential decreasing of photon flux which is inversely proportional to position x and the absorption coefficient α of the solar cell (see Equations 3, 4 and 6).

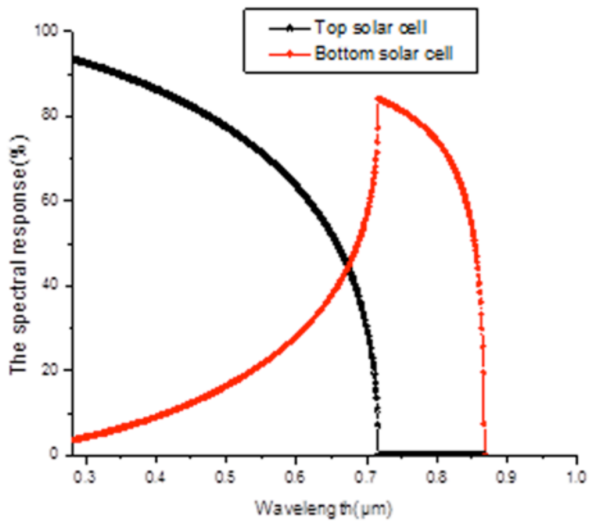

Fig. 2.The spectral response for the two solar cells.

These remarks allow the distribution of each wavelength range suitable to each cell, then to calculate the appropriate photocurrent.

3.2. The bandgap optimization

Now, by varying x in formula of AlxGa1-xAs/GaAs material composition, the energy gap varies therefore, the spectral response of the two cells and their photocurrent change as well. The following figure shows the variation of the photocurrent density of each cell depending on the bandgap of the top cell despite keeping the bottom's cell bandgap Eg2 constant (1.42 eV).

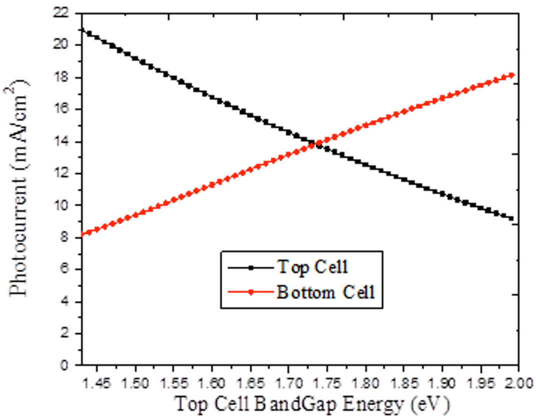

Fig. 3. The variation of photocurrent density versus top cell bandgap, the bottom bandgap remains fixed (Eg_2= 1.42eV).

The two cells are connected in series so the total solar cell current is the smallest [18]. The aim of this optimization is to increase the total solar cell current. Figure 3 shows that for low bandgap the photocurrent of the top cell decrease while the photocurrent of the bottom cell increases. The principal cause of this result is owing to the spectral response behavior of each cell (see Fig.2). The optimum value of J_{ph} is the intersection of the two currents which corresponds to sameness photocurrent. This means that the optimum of top cell bandgap is Eg_1 = 1.733eV. This value permits the achievement of optimal photocurrent density of 13.81mA/cm^2 thereby give a better efficiency of the tandem solar cell. This value of bandgap corresponds to a fraction of Al of about 20% according to the equation (7) taken from the experimental data for Eg of Aspnes et al. [19] and Aubel et al. [20].

$$E_g(x) = 1.430 + 1.707x - 1.437x^2 + 1.310x^3 \\ = 1.430 + 1.580x + x(1-x)(0.127 - 1.310x) \quad (7)$$

$E_g(x)$ present the lowest direct bandgap versus x for $Al_xGa_{1-x}As/GaAs$.

Figure 4 shows the variation of the efficiency of tandem solar cell according to the variation of the bandgap of the top cell.

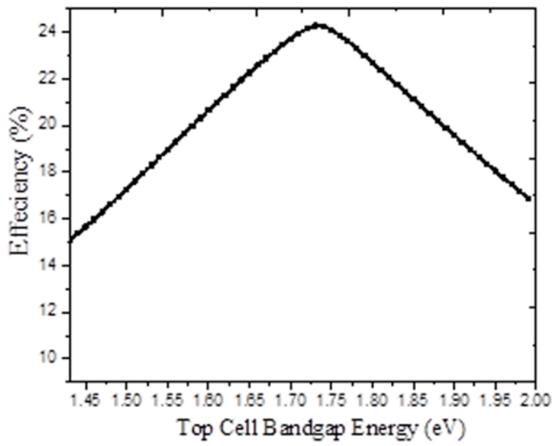

Fig. 4. The variation of efficiency versus top cell bandgap, the bottom cell bandgap remains fixed (Eg_2= 1.42eV).

The maximum efficiency of about 24.3% corresponds to top cell bandgap of Eg_1 = 1.733eV already found in figure 3.

3.3. The top solar cell thinness optimization

After having obtained the optimum value of top solar cell bandgap, the emitter's thickness effect on the photocurrent of the both solar cells is investigated.

By the same optimization policy, we tend to improve the photocurrent by varying the top cell thickness, this allows more photon absorption. Figure 5 shows the variation of photocurrent density versus the top cell thickness while keeping the bottom's cell thickness constant (X2=2.5µm).

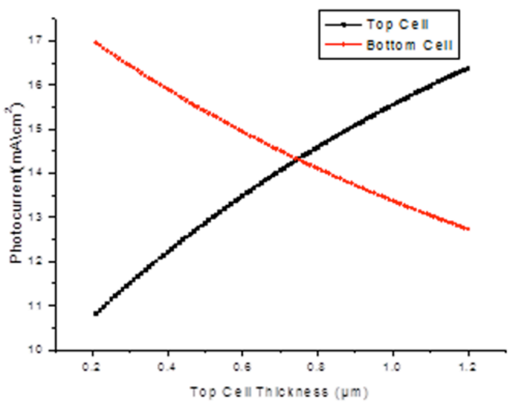

Fig. 5. The variation of photocurrent density versus top cell thickness, the bottom thickness remains fixed (X_2= 2.5µm).

From the intersection of the photocurrent density curves of the top cell and bottom one of Fig.5 the optimum value of thickness is almost 0.747µm which engenders a photocurrent density of 14.33mA/cm^2. There is an improvement of photocurrent of about 3.6%.

Other authors [21] found the optimum $Al_xGa_{1-x}As$ layer thicknesses of 10 µm for the emitter in $Al_xGa_{1-x}As/GaAs$ heterojunction solar cell.

In this study $Al_xGa_{1-x}As$ constitutes a top layer cell counter to other work [22] in which $Al_xGa_{1-x}As$ is used as surface barrier layer or as windows layer [23, 24].

The figure 6 shows the variation of efficiency against top cell thickness while keeping the bottom's cell thickness constant (X_2=2.5µm).

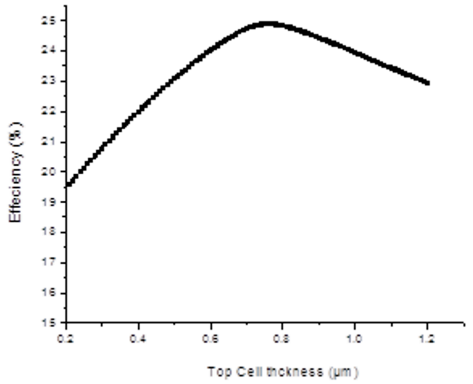

Fig. 6. The variation of efficiency versus top cell emitter thickness, the bottom thickness remains fixed (X_2= 2.5µm).

From Fig.6 it is seen that the efficiency improves to a maximum of 24.9% for a thickness of 0.747 µm, already found in figure 5, an increase of 2.4%.

4. Conclusions

An optimization of AlGaAs/GaAs top solar cell emitter's bandgap thickness in order to limit losses and improve efficiency in the MJSC has been introduced. A photocurrent density of 13.81mA/cm^2 and an efficiency of about 24.3% have been obtained after the top cell bandgap optimization. These two values are boosted, after the emitter thickness optimization, to about 3.6% and 2.4% to reach 14.33mA/cm^2 and 24.9% respectively. The optimum emitter bandgap and thickness values are 1.73 eV and 0.747µm respectively. As a perspective, the study of the solar cell efficiency for sun concentration system and the effect of window layer on photocurrent could be also taken into account.

Acknowledgements

The authors are grateful to Mr. Djamel Ghafour from ENPO Oran for his contribution and to Mr. Attaoui Abdelbari from UTMB Bechar for his guidance and his review of paper's English.

References

[1] M. Dhankhar, O. Pal Singh, V.N. Singh, "Physical principles of losses in thin film solar cells and efficiency enhancement methods", Renewable and Sustainable Energy Reviews, vol. 40, pp. 214-223, 2014.

[2] T. Frijnts, S. Kühnapfel, S. Ring, O. Gabriel, S. Calnan, J. Haschke, B. Stannowski, B. Rech, R. Schlatmann, "Analysis of photo-current potentials and losses in thin film crystalline silicon solar cells", Solar Energy Materials and Solar Cells,vol.143, pp. 457-466, 2015.

[3] M. Berginski, J. Hüpkes, A. Gordijn, W. Reetz, T. Wätjen, B. Rech, M. Wuttig, "Experimental studies and limitations of the light trapping and optical losses in microcrystalline silicon solar cells", Solar Energy Materials and Solar Cells, vol. 92, pp. 1037-1042, 2008.

[4] M. Limpinsel, A. Wagenpfahl, M. Mingebach, C. Deibel, and V. Dyakonov, "Photocurrent in bulk heterojunction solar cells", Phys. Rev. Vol. B 81, pp. 085203, 2010.

[5] A. P. Kirk and M. V. Fischetti, "Fundamental limitations of hot-carrier solar cells", Phys. Rev, Vol. B 86, pp. 165206, 2012.

[6] S. Saylan, T. Milakovich , S. Abdul Hadi, A. Nayfeh, Eugene A. Fitzgerald, Marcus S. Dahlem, "Multilayer antireflection coating design for GaAs0.69P0.31/Si dual-junction solar cells", Solar Energy, Vol. 122, pp.76–86, 2015.

[7] M.A. Green, K. Emery, Y. Hishikawa, W. Warta," Solar cell efficiency tables (version 44)", Prog. Photovolt. Vol. 22, pp. 701-710, 2014.

[8] H. Tan, P. Babal, M. Zeman, A. H.M. Smets,"Wide bandgap p-type nanocrystalline silicon oxide as window layer for high performance thin-film silicon multi-junction solar", Solar Energy Materials and Solar Cells, Vol.132, pp. 597-605, 2015.

[9] N. López, L. A. Reichertz, K. M. Yu, K. Campman, and W. Walukiewicz, "Engineering the Electronic Band Structure for Multiband Solar Cells", Phys. Rev. Lett, Vol. 106, pp. 028701, 2011.

[10] S. Kim, S. Kasashima, P. Sichanugrist, T. Kobayashi, T. Nakada, M. Konagai, "Development of thin-film solar cells using solar spectrum splitting technique", Solar Energy Materials and Solar Cells,Vol.119, pp.214–218, 2013.

[11] R. R. King, D. Bhusari, A. Boca, D. Larrabee, X.-Q. Liu, W. Hong, C. M. Fetzer, D. C. Law, and N. H. Karam, "Band gap-voltage offset and energy production in next-generation multijunction solar cells", 25th European Photovoltaic Solar Energy Conference, Valencia, Spain, Sep. 6-10. pp. 33-47, 2010.

[12] R. R. King, D. C. Law, K. M. Edmondson, C. M. Fetzer, G. S. Kinsey, H. Yoon, R. A. Sherif, and N. H. Karam, "40% efficient metamorphic GaInP⁄GaInAs⁄GeGaInP⁄GaInAs⁄Ge multijunction solar cells",Appl Phys Lett, Vol. 90, pp. 183516, 2007.

[13] A. Le Bris, J. Rodiere, C. Colin et al, "Hot Carrier Solar Cells: Controlling Thermalization in Ultrathin Devices", IEEE Journal of Photovoltaics, Vol. 2 pp. 506-511, Oct 2012.

[14] Goldberg Yu. A, M. Levinshtein, S. Rumyantsev and M. Shur, Handbook Series on Semiconductor Parameters, 1st ed., vol.2. London: World Scientific, 1999, pp. 1-36.

[15] S.Adachi, “GaAs, AlAs, and Al x Ga1−x As: Material parameters for use in research and device applications”, J. Appl. Phys, Vol. 58, pp.R1-R29, 1985.

[16] E. Lorenzo, Solar Electricity: Engineering of Photovoltaic System, 1st ed., Sevilla: Progensa,1994,ch. 2.

[17] J.N. Shive, The properties, physics, and design of Semiconductor Devices, Princeton, New Jersey: Van Nostrand, 1959, ch. 2.

[18] Sarah R. Kurtz, P. Faineand J. M. Olson, “Modeling of two- junction, series- connected tandem solar cells using top- cell thicknessas an adjustable parameter”, J. Appl. Phys,Vol.68, pp.1890, 1990.

[19] D. E. Aspnes, S. M. Kelso, R. A. Logan, and R. Bhat, “Optical properties of Al x Ga1−x As”, J. Appl. Phys, Vol. 60, pp.754-767, 1986.

[20] J. L. Aubel, U. K. Reddy, S. Sundaram, W. T. Beard, and J. Comas, “Interband transitions in molecular- beam- epitaxial Al x Ga1−x As/GaAs”, J. Appl. Phys,Vol.58, pp. 495-498, 1985.

[21] J. Zou, Y. Zhang, W. Deng, X. Peng, S. Jiang, and B. Chang, “Effects of graded band-gap structures on spectral response of AlGaAs/GaAs photocathodes”, Applied Optics, Vol. 54, pp. 8521-8525, 2015.

[22] H. Urabe, M. Kuramoto, T. Nakano, A. Kawaharazuka, T. Makimoto, Y. Horikoshi, “Effects of surface barrier layer in AlGaAs/GaAs solar cells”, Journal of Crystal Growth, Vol. 425, pp. 330–332, 2015.

[23] M. Abderrezek, F. Djahli, M. Fathi, M. Ayad, “Numerical Modeling of GaAs Solar Cell Performances”, Elektronika ir Elektrotechnika, Vol. 19, pp.41-44, 2013.

[24] S. Khelifi et A. Belghachi, “Le Rôle de la Couche Fenêtre dans les Performances d’une Cellule Solaire GaAs”, Rev. Energ. Ren, Vol.7, pp. 13-21, 2004.